

# MODELING HIGH TEMPERATURE FLOW BEHAVIOR OF AN AL 6061 ALUMINIUM ALLOY

E. Badami\* , M. T. Salehi and S. H. Seyedein

\* Badami\_e@iust.ac.ir

Received: April 2014

Accepted: August 2014

School of Metallurgy and Materials Engineering, Iran University of Science and Technology, Tehran, Iran.

**Abstract:** Hot deformation behavior of a medium Cr/Mn Al6061 aluminum alloy was studied by isothermal compression test at temperatures range of 320 to 480 °C and strain rates range of 0.001 to 0.1 s<sup>-1</sup>. The true stress-true strain curves were analyzed to characterize the flow stress of Al6061. Plastic behavior, as a function of both temperature and strain rate for Al6061, was also modeled using a hyperbolic sinusoidal type equation. For different values of material constant  $a$  in the range of 0.001 to 0.4, values of  $A$ ,  $n$  and  $Q$  were calculated based on mathematical relationships. The best data fit with minimum error was applied to define constitutive equation for the alloy. The predicted results of the proposed model were found to be in reasonable agreement with the experimental results, which could be used to predict the required deformation forces in hot deformation processes.

**Keywords:** Al6061 Aluminium Alloy, Hot Deformation, Constitutive Equations.

## 1. INTRODUCTION

The 6XXX series aluminum alloys (Al-Mg-Si based) with the main strengthening phases of Mg<sub>2</sub>Si are widely applied in automotive and construction industries due to their favorable corrosion resistance, welding ability, low scrap compatibility and low cost. Cr and Mn are added to these alloys to increase their strength and control the grain size [1].

During thermo-mechanical processes, high temperature behavior of metallic materials is always accompanied by various interconnecting metallurgical phenomena such as work hardening, dynamic recovery (DRV), dynamic recrystallization (DRX) and flow instability.

Constitutive equations including an Arrhenius term have been commonly applied for various materials with the objective of the hot deformation process behavior and defining the physical mechanisms that control the deformation [2].

Investigating the hot temperature behavior & driving material constants in Constitutive equations have been the subject of many researches for different alloys [2-8], including aluminium alloys [9,10,11,12]. In spite of its widely industrial application, a few researchers considered driving constants for AA 6061 aluminium alloy [13].

Y. Li and T. G. Langdon investigated the creep behavior of an Al 6061-Al<sub>2</sub>O<sub>3</sub> composite [10] Spigarelli et al. analyzed Constitutive equations for hot deformation of an Al 6061-20 vol. % Al<sub>2</sub>O<sub>3</sub> composite [11]. McQueen and Ryan, studied the hot deformation behavior of a Pre-aged 6061 alloy [5]. The isothermal compression of low Cr/Mn Al6061 was investigated at temperatures in the range of 300 to 450 °C and strain rates range of 0.5 to 30 1/s by Chunlei et al. [13]. The Constants derived by Chunlei et al. [13] are influenced by high strain rates of experiments while essentially constitutive equations describe the material behavior during creep process which strain rates are low.

In this study, hot compression behavior of a medium Cr/Mn Al6061 considered, conducting experiments at temperature range of 320 to 480 °C and strain rate range of 0.001 to 0.1 1/s. The material behavior has been modeled by constitutive equations based on the experimental data and it was evaluated using relative error (R), average absolute relative error (AARE) and average root mean square error (RMSE).

## 2. EXPERIMENTAL PROCEDURE

The material investigated in the present study was a commercial Al6061. the chemical composition of alloy is given in Table 1.



**Table 1.** Chemical composition of AA6061

Si	Mg	Fe	Mn	Cu	Cr	Ni	Zn
0.68	0.96	0.18	0.008	0.32	0.13	0.01	0.09
Sn	V	Co	Bi	B	Cd	Pb	Al
<0.005	0.004	<0.002	<0.004	0.002	0.002	Trace	97.61

An extruded billet from the material was homogenized in a laboratory furnace for 3 hours at a temperature of 550 °C and cooled down to room temperature in the furnace. The resulting microstructure is shown in Figure 1, which consists of equi-axed grains with a size of about 130 μm.

The cylindrical specimens with a height of 15 mm and a diameter of 10 mm were machined from the billet after homogenization.

The compression tests were carried out according to ASTM E209 standard [14] using an Instron-4208 universal testing machine equipped with a programmable resistance furnace. A high accuracy load cell (model: SSM-DJM-20 kN) with the capability of measuring load forces down to 0.1 kg was employed to record the stress

values. Variations of stress and strain were continuously monitored through an appropriate data acquisition system.

The specimens were preheated up to the test temperatures and kept for 7 minutes to allow for thermal homogenization before starting the test. The deformation temperature was measured by thermocouples which were welded to the center region of the specimen surface.

The specimens were then hot compressed up to the strain of 0.6. A very thin mica plate was used to minimize friction effect and also prevent adhesion of the specimen on the die.

### 3. RESULTS AND DISCUSSION

Figure 2 shows true stress–true strain curves of the experimental alloy obtained from compression tests at temperatures range of 320 to 480 °C under strain rates of 0.001, 0.01, and 0.1 1/s, respectively.

General characteristics of the flow curves are similar in all of the deformation conditions. That is, flow stress rises to a plateau followed by a constant or steady state flow stress over the strain range of 0.05 to 0.6.

In metals of high stacking fault energy, such as aluminum and its alloys,  $\alpha$ -iron and ferritic steels,

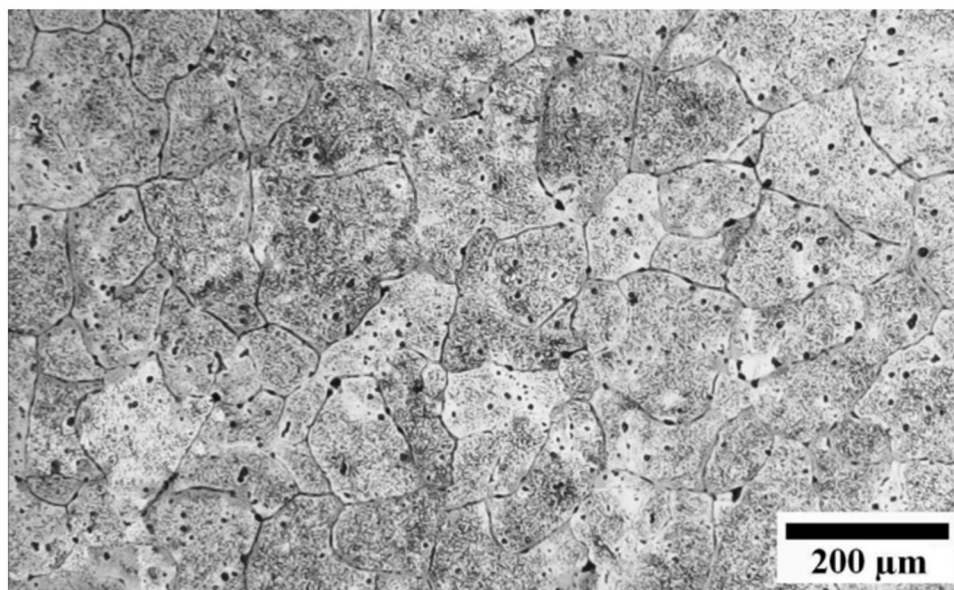


**Fig. 1.** Microstructure of homogenized material.

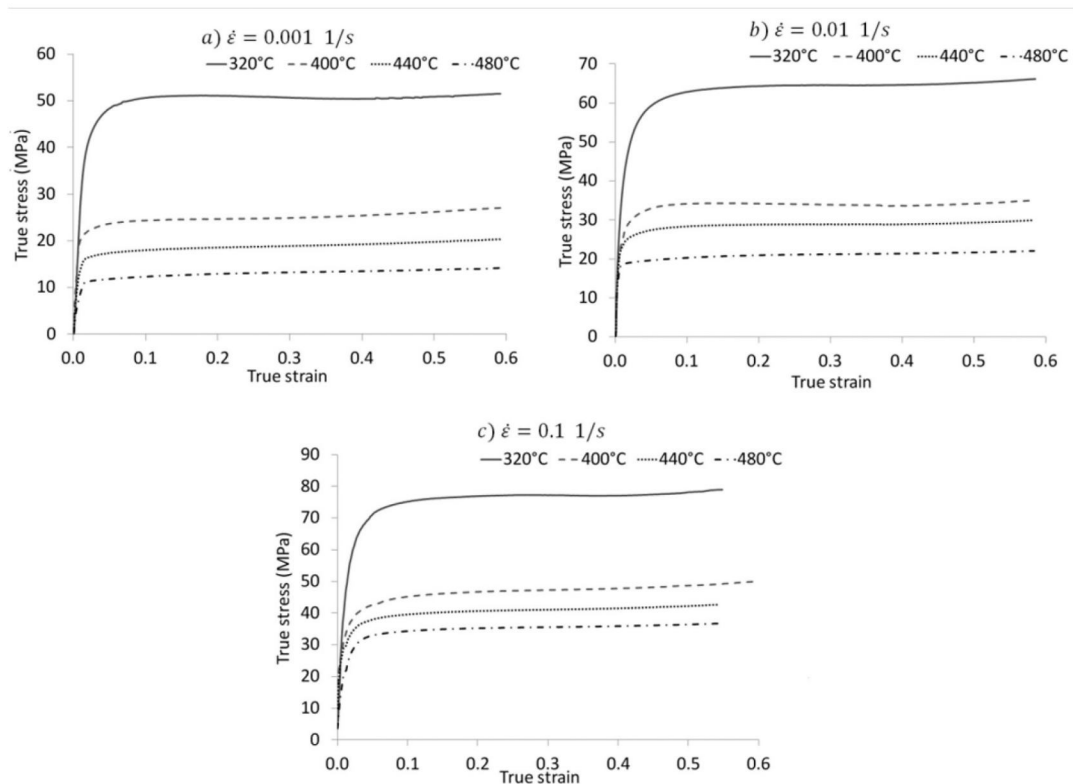


**Fig. 2.** The true stress–true strain curves of Al 6061 alloy obtained from hot compression tests in the temperature range of 320–480 °C and strain rates of (a) 0.1, (b) 0.01 and (c) 0.001.

dislocations climb and cross-slip occurs readily. The dynamic recovery is therefore rapid and extensive at high temperatures [15,16,17]. Thus, such behavior from this grade of aluminum alloy 6061 indicated that the alloy did not present strain hardening in the studied range of temperatures and strain rates. During the thermo-mechanical processes of this alloy, recovery process completely balanced the effects of straining and work hardening.

the error of experiments defined by repeating the test at same condition.

The effect of deformation temperatures and strain rates on flow stress is demonstrated in Figure 3. The flow stress at constant true strain value of 0.1 was plotted as a function of the deformation temperature and strain rate in Figure 3-a and b, respectively. It can be seen that the flow stress is sensitive to both the temperature and strain rate.

The flow stress decreased with increasing temperature at a constant strain rate.

Increasing deformation temperature by 160 °C from 320 to 480 °C decreased flow stress by approximately one-fifth, one third and one half in the strain rates of 0.001, 0.01 and 0.1, respectively, which demonstrates that temperature had higher influence on flow stress in lower strain rates.

Strain rate value of 0.1 per sec is typical of hydraulic presses in hot deformation processes of Al alloys. The low flow stress in the strain rates of hydraulic pressing enables finer details in forged parts than those obtained in mechanical presses or hammers [18]. Therefore, the selection of the forging temperature has a critical effect on the ease of material flow. However, due to the heat generated by the deformation process, the use of high preheat temperatures for forging create a risk in the development of the hot shortness (i.e., sever cracking) due to the incipient melting.

It can also be seen in Figure 3-b that the increase of temperature intensifies the influence



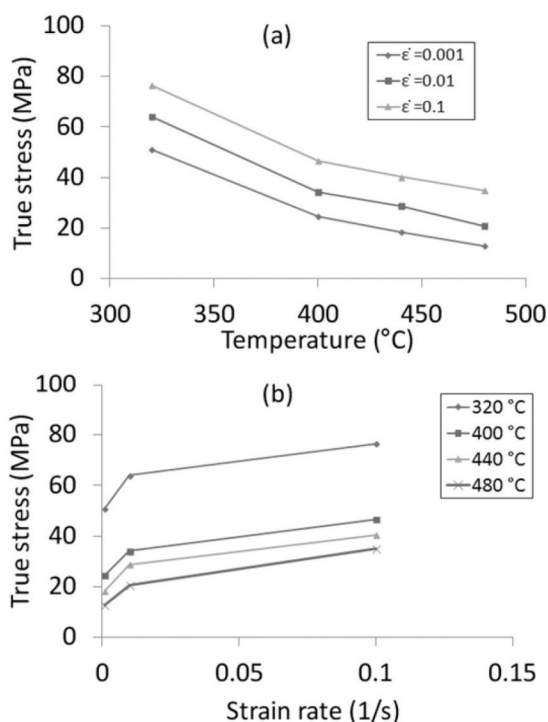


**Fig. 3.** Influence of the experimental parameters on the flow stress at a true strain of 0.1. (a) effect of temperature and (b) effect of strain rate.

of strain rate on flow stresses. Increase of strain rate value from 0.001 to 0.1 also leads to the increase of the flow stress by approximately 1.5 times at 320 °C and about 3 times at 480 °C.

#### 4. DEFORMATION CONSTITUTIVE EQUATIONS

Constitutive equation is often cited to model the deformation process response between the temperature, strain and strain rate values in the hot working process of metals.

The flow stress data obtained from the compression tests under different strain rates and temperatures can be used to determine the material constants of constitutive equations.

In this study, based on the obtained experimental data, a hyperbolic sine law was introduced to model the flow stress of Al6061 under constant strain rates ranging from 0.001 to 0.1 s<sup>-1</sup> and at temperatures varying from 320 to 480 °C.

The temperature and strain rate dependence of

the flow stress in hot deformation process condition is generally expressed by the hyperbolic sine law as follows [19]:

$$\dot{\epsilon} = A(\text{Sinh}(\alpha \sigma_f))^m \left( -\frac{Q_{\text{def}}}{R_0 T_{\text{def}}} \right) \quad (1)$$

where A, n and  $\alpha$  are material constants,  $\dot{\epsilon}$  is the strain rate (1/s),  $\sigma$  is the flow stress (MPa), Q is the deformation activation energy (kJ/mol), R<sub>0</sub> is the gas constant (kJ/molK<sup>-1</sup>) and T is the temperature (K).

The stress multiplier  $\alpha$  is an additional adjustable constant which brings  $\alpha\sigma$  into the correct range to make the constant T curves in  $\ln(\dot{\epsilon})$  versus  $\ln[\text{sinh}(\alpha\sigma)]$  plots to be linear and parallel [5].

Considering the logarithm of both sides of the above equation it leads to:

$$\ln[\text{sinh}(\alpha\sigma)] = \frac{\ln(\dot{\epsilon})}{n} + \frac{Q}{nRT} - \frac{\ln A}{n} \quad (2)$$

The slope of  $\ln[\text{sinh}(\alpha\sigma)]$  versus  $\ln(\dot{\epsilon})$  yields 1/n and, for a particular strain rate, differentiating Eq. (2) presents:

$$Q = Rn \frac{d\{\ln[\text{sinh}(\alpha\sigma)]\}}{d(1/T)} \quad (3)$$

where the values of  $\alpha$ , A, n and Q cannot be directly determined using the linear statistical regression models because there are four constants of  $\alpha$ , A, n and Q in Eq. (2). In order to calculate the values of A, n and Q, first, a constant value of  $\alpha$  was considered and then values of A, n, Q were calculated. The result was quantified by employing the relative error (R) as follows:

$$R = \frac{\sum_{i=1}^N (E_i - \bar{E})(P_i - \bar{P})}{\sqrt{\sum_{i=1}^N (E_i - \bar{E})^2 \sum_{i=1}^N (P_i - \bar{P})^2}} \quad (4)$$

where  $E_i$  and  $P_i$  are the experimental finding and predicted value, respectively; E and P are mean

values of  $E_i$  and  $P_i$ , respectively, and  $N$  is the total number of the employed data in the investigation.

It should be noted that the higher value of  $R$  may not always indicate a better performance of a model because of the tendency of the equation to be biased towards the higher or lower values [3]. Hence, the average absolute relative error (AARE) and average root mean square error (RMSE) are also calculated as follows [20]:

$$AARE (\%) = \frac{1}{N} \sum_{i=1}^N \left| \frac{E_i - P_i}{E_i} \right| \times 100 \quad (5)$$

$$RMSE = \sqrt{\frac{1}{N} \sum_{i=1}^N (E_i - P_i)^2} \quad (6)$$

Variation of the error values for different values of  $\alpha$  is shown in Figure 4. From the comparison of these curves the optimum value of  $\alpha$  is selected, which is then substituted in Eq. (1). The optimum value for  $\alpha$  in these experiments is  $0.052 \text{ MPa}^{-1}$ .

The value of  $\alpha$  is an indicative of a material's intrinsic ability to resist deformation; the more the resistance of a material to deformation, the lower its value for  $\alpha$  would be [19].

Compared to a value of  $\alpha$  obtained for a low

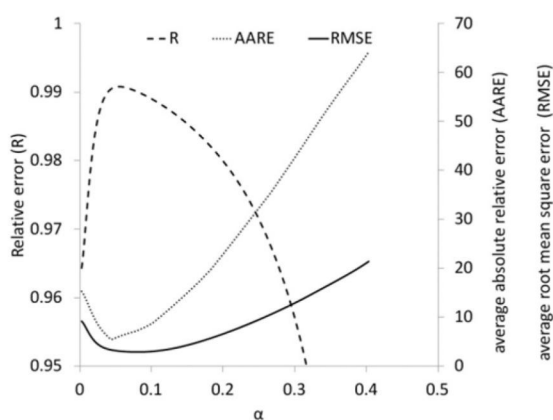


Fig. 4. Change of error values with  $\alpha$ .

Cr/Mn Al6061 (as  $0.01 \text{ MPa}^{-1}$ ) [13], the value of  $\alpha$  was significantly higher here. However, this difference could not be considered a sign of a higher resistance of the material to deformation. This difference was essentially because of a significantly higher strain rates in G. Chunlei et al.'s [13] study, which resulted in higher value for the flow stresses.

The value of  $0.052$  for  $\alpha$  is fairly common for Al alloys [19]. When the value of the term  $\alpha\sigma$  is less than  $0.8$  the hyperbolic sine law approximates to power law and when it is greater than  $1.2$ , the hyperbolic sine law approximates to power-law breakdown regime [19]. As the value of  $\alpha\sigma$  in this study is in the range of  $0.65$  to  $\sim 4$ , none of power law or power-law breakdown regimes can be chosen and the sinh equation should be applied across this broad range of  $\alpha\sigma$  in this study.

The values of  $A$ ,  $n$  and  $Q$  in Eq. (3) can now be obtained from using a linear regression method.

Since the flow stress was in a steady state during the test in the studied range of the temperatures and strain rates, it can be assumed that the strain had no influence on constitutive equation constants. Thus, the material constants (i.e.,  $A$ ,  $n$  and  $Q$ ) are independent from that the strain.

Isothermal plot of  $\ln[\sinh(\alpha\sigma)]$  versus  $\ln(\dot{\epsilon})$  at various deformation process temperatures is

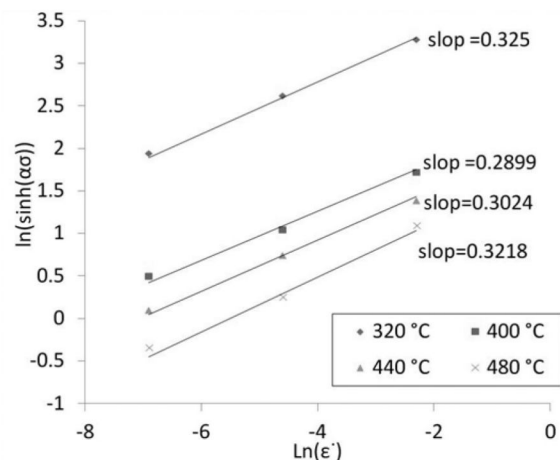


Fig. 5. Isothermal plot of  $\ln[\sinh(\alpha\sigma)]$  vs.  $\ln(\dot{\epsilon})$  at various deformation temperatures



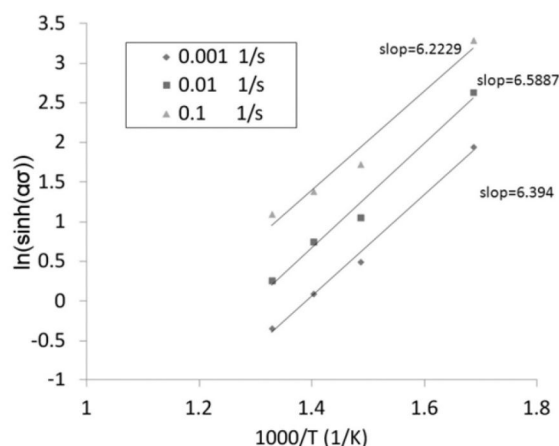


Fig. 6. Plot of the  $\ln[\sinh(\alpha\sigma)]$  data as a function of the inverse of temperature.

represented in Figure 5, which shows an average value of 3.22 for  $n$ .

The value of  $n$  decreases almost inversely with the value of  $\alpha$  parameter [5].

Comparison of the results for values of  $\alpha$  and  $n$  in this study with those in G. Chunlei et al.'s study [13] are confirmed in this relationship.

With a constant strain rate, the logarithmic plot of the flow stress as an inverse function of the temperature produced linear curves with slopes of equal to  $Q/nR$  (see Figure 6). According to the regression analysis of the data, the activation energy was determined to be at 171.38 kJ/mol in different strain values at temperatures in the range of 320 to 480°C.

This value of activation energy is larger than any imagined atomic mechanism. While this value may be considered apparent, but the value of activation energy provides a simple statement about how rapidly the flow stress changes over the temperature range.

McQueen and Ryan, reported an activation energy of 205 kJ/mol for a Pre-aged 6061 alloy [5].

Y. Li and T. G. Langdon [10] reported the value of 150 KJ/mole for shear creep of the Al 6061-20 vol. %irregularly shaped  $Al_2O_3$  composite in the temperature range of 350 to 500 °C. The value of  $Q \approx 125$  kJ/mol obtained in the Al 6061-20 vol. %spherical  $Al_2O_3$  composite after creep testing in tension in the temperature range

of 200-400 °C [10]. Y. Li and T. G. Langdon [10] concluded that creep of the Al 6061-20 vol. %  $Al_2O_3$  composite controlled by the viscous glide of dislocations dragging Mg atom atmospheres.

Spigarelli et al. [11] calculated the values of 5.6 for stress exponent and 150 KJ/mol for activation energy from hot torsion test of an Al 6061-20 vol. %  $Al_2O_3$  composite. They concluded the mechanism controlling hot deformation and creep at high stresses is the climb of dislocations.

Comparison of the obtained activation energy in this study with that in the Spigarelli et al.'s study [11] could be misleading due to the difference in the value of  $\alpha$ .

The analogy between the  $n$  and  $Q$  values for this alloy with typical values of these parameters for solid solution alloys confirms that the viscous glide of dislocations and dragging an atmosphere of solute atoms is the rate-controlling process.

The calculated value of  $Q$  in this study is about 20% higher than the activation energy for self-diffusion in Al (~143.4 kJ/mol [10,21]) or diffusion of Mg atoms in Al (~ 130.5kJ/mol [10,21]).

It is quite obvious that slightly higher value of activation energy activation energy respect to pure Al are mainly due to a presence of Cr and Mn and different distribution of secondary phase precipitates ( $Mg_2Si$ ) and dispersoids formation. The alloy considered in this study is solution treated and slowly cooled, giving a sort of aged structure. High temperature testing, due to the relatively short heating times, could cause minor variation in the precipitate distribution.

Cr and Mn in 6XXX series aluminum alloys also lead to the formation of the dispersoids during heating to homogenization temperatures. They improve the properties of the alloy by increasing resistance to the recrystallization process [22]. Higher activation energy in the studied aluminum alloy in this research is correlated to the contents of the solutes, secondary phase precipitates and dispersoid elements.

Activation energy is higher in alloys with increased value of solute, which becomes more effective at low temperatures either as atmospheres is immobilized or through the



strengthening of the impurity particles [19]. Such a behavior can be seen in Figure 6, in which the slope of curves increases with the decrease in temperature at constant strain rates and results in higher activation energy in the alloy at lower values of the temperature. Thus, it may be stated that the presence of modifying elements including Cr and Mn in the alloy could increase hot deformation activation energy by increasing the solute content, secondary phase precipitates and dispersoid and results in higher flow stresses. This process also causes that the flow stress of the alloy to be more sensitive to temperature changes.

The value of  $2.83 \times 10^9$  was obtained for the constant term A based on the above data.

The predicted values of the flow stress are plotted against the experimental flow stress values in Figure 7. This figure shows comparison of model prediction with experiments. Accordingly, it shows that the agreement between the measured and calculated values was satisfactory. The model is more accurate at lower strain rate and higher temperatures. As it can be seen the worst case is related to the test with strain rate of 0.1 1/s and 320 °C. it can be result of change in controlling mechanism of deformation. Referring to Figure 6 reveals that the activation energy is higher at lower temperatures and higher strain rates. In fact, immobilization of atmosphere or strengthening of the impurity particles cause change in controlling mechanism and make the model to deviate from the experimental data. At high temperatures, dislocations acquire a new degree of freedom. They can climb as well as glide. If a gliding dislocation is held up by discrete obstacles, a little climb may release it, allowing it to glide to the next set of obstacles where the process is repeated. The glide step is responsible for almost all of the strain, although its average velocity is determined by the climb step. Mechanisms which are based on this climb-plus-glide sequence will be referred to as climb-controlled creep. The important feature which distinguishes these mechanisms from earlier is that the rate-controlling process, at an atomic level, is the diffusive motion of single ions or vacancies to or from the climbing dislocation,

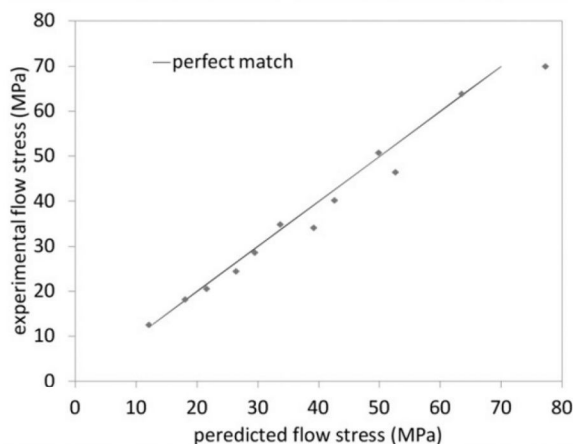


Fig. 7. Correlation between experimental and predicted flow stresses of studied Al 6061 alloy.

rather than the activated glide of the dislocation itself.

The value of the relative error ( $R = 0.9908$ ) demonstrates good correlation between the experimental and predicted results.

Values of AARE and RMSE were 5.88% and 3.214, respectively, indicating good accuracy of the predicted flow stresses based on the proposed constitutive equation.

Eq. (1) can be written as follows:

$$\sigma = \frac{1}{\alpha} \left\{ \left( \frac{Z}{A} \right)^{\frac{1}{n}} + \sqrt{\left( \frac{Z}{A} \right)^{\frac{2}{n}} + 1} \right\} \quad (7)$$

where Z is Zener–Hollomon parameter and is defined as:

$$Z = \dot{\epsilon} \exp[Q/RT] \quad (8)$$

Substituting for the constant parameters in the Eqs. 7 and 8 produces the following equation for high temperature flow behavior of a medium Cr/Mn Al6061 aluminum alloy:

$$\sigma = \frac{1}{0.052} \left\{ \left( \frac{Z}{2.83e9} \right)^{\frac{1}{3.22}} + \sqrt{\left( \frac{Z}{2.83e9} \right)^{\frac{2}{3.22}} + 1} \right\} \quad (9)$$

where

$$Z = \dot{\epsilon} \exp[171.38/RT] \quad (10)$$



## 5. CONCLUSIONS

Isothermal hot compression tests were employed to study the high temperature flow behavior of a medium Cr/Mn Al6061 aluminium alloy at the temperature range of 320 to 480 °C and strain rates range of 0.001 to 0.1. It was found that the flow stress level was significantly affected by the strain rate and deformation temperature. The material presented a steady state flow behavior. A dynamic recovery process was probably occurred which completely balanced the effects of straining and work hardening in the given ranges of the temperature and strain rate.

The effects of the temperature and strain rate on the flow stress were represented by a hyperbolic sinusoidal type equation.

The value of the parameter  $\alpha$  in these experiments was  $0.052 \text{ MPa}^{-1}$  and the values of the constants A, n and Q were  $2.83 \times 10^9$ , 3.22 and  $171.38 \text{ kJ/mol}$ , respectively, and they were independent of the strain value.

Results show that viscous glide of dislocations and dragging an atmosphere of solute atoms is the rate-controlling process.

The average absolute relative errors and absolute values of average root mean square error for the model were 5.88% and 3.214, respectively.

## ACKNOWLEDGEMENTS

The authors acknowledge Mr. H. R. Abedi for providing valuable discussions.

They also are grateful to Mrs. A. Paryani for her help in analyzing the data.

## REFERENCES

1. Smith, W. F., "Structure and Properties of Engineering Materials": McGraw-Hill, 1987.
2. Mirzadeh, H., Cabrera, J. M., & Najafizadeh, A. "Modeling and Prediction of Hot Deformation Flow Curves," METALLURGICAL AND MATERIALS TRANSACTIONS A, vol. 43A, pp. 108-123, 2012.
3. Sabokpa, O., Zarei-Hanzaki, V., Abedi, H. R., Haghdadi, N., "Artificial neural network modeling to predict the high temperature flow behavior of an AZ81 magnesium alloy," Materials and Design, vol. 39, pp. 390-396, 2012.
4. Morakabati, M., Aboutalebi, M., Kheirandish, Sh., Karimi Taheri, A., & Abbasi, S. M., "High temperature deformation and processing map of a NiTi intermetallic alloy," Intermetallics, vol. 19, pp. 1399-1404, 2011.
5. McQueen, H. J., & Ryan, N. D., "Constitutive analysis in hot working," Materials Science and Engineering A, vol. 332, pp. 43-63, 2002.
6. Spigarelli, S., "Constitutive Equations in Creep of the AE44 Magnesium Alloy," Materials Science Forum, vol. 604-605, pp. 357-365, 2009.
7. Liu, L., & Ding, H., "Study of the plastic flow behaviors of AZ91 magnesium alloy during thermomechanical processes," Journal of Alloys & Compound, vol. 56, pp. 484-949, 2009.
8. Samantaray, D., Mandal, S., & Bahaduri, A. K., "Constitutive analysis to predict high temperature flow stress in modified 9Cr-1Mo (P91) steel," Material & design, vol. 31, pp. 981-984, 2010.
9. Rezaei Ashtiani, H. R., Parsa, M. H., Bisadi, H., "Constitutive equations for elevated temperature flow behavior of commercial purity aluminum," Materials Science and Engineering: A, vol. 545, pp. 61-67, 2012.
10. Li, Y., & Langdon, T. G., "Creep Behavior of an Al-6061 Metal Matrix Composite Reinforced With Alumina Particulates," Acta mater., vol. 45, no. 11, pp. 4797-4806, 1997.
11. Spigarelli, S., Evangelista, E., Cerri, E. & Langdon, T. G., "Constitutive equations for hot deformation of an Al-6061/20%Al<sub>2</sub>O<sub>3</sub> composite," Materials Science and Engineering A, vol. 319-321, pp. 721-725, 2001.
12. Haghdadi, N., Zarei-Hanzaki, A., & Abedi, H. R., "The flow behavior modeling of cast A356 aluminum alloy at elevated temperatures considering the effect of strain," Material Science Engineering, vol. 7, pp. 535-252, 2012.
13. Chunlei, G., Yongdong, X., & Mengjun, W., "Prediction of the flow stress of Al6061 at hot deformation conditions," Materials Science and Engineering A, vol. 528, pp. 4199-4203, 2011.
14. "Standard practice for compression tests of



- metallic materials at elevated temperatures with conventional or rapid heating rates and strain rates.," Annual Book of ASTM Standards, vol. 03.01, 2010.
15. Humphreys, F. J., & Hatherly, M., *Recrystallization and Related Annealing*. Oxford: Elsevier Ltd, 2004.
  16. De Pari, L., Wojciech, Jr., Misiolek, Z., "Theoretical predictions and experimental verification of surface grain structure evolution for AA6061 during hot rolling," *Acta MATERIALIA*, vol. 56, pp. 6174–6185, 2008.
  17. Gourdet, S., Konopleva, E. V., McQueen, H. J., Montheillet, F., "Recrystallisation during hot deformation of aluminium," *Materials Science Forum*, vol. 217 - 222, pp. 441-446, 1996.
  18. Totten, G. E., & MacKenzie, D., S., *Handbook of Aluminum, Physical Metallurgy and Processes*. NEW YORK: MARCEL DEKKER, INC., 2003.
  19. McQueen, H. J., Spigarelli, S., & Kassner, M. E., "Hot Deformation and processing of Aluminium alloys": CRC press, 2011.
  20. Rokni, M. R., Zarei-Hanzaki, A., Roostaei, A., Abolhasani, A., "Constitutive base analysis of a 7075 aluminum alloy during hot compression testing," *Material & Design*, vol. 32, pp. 4955–4960, 2011.
  21. Hsiao, I. C., & Huang, J. C., "Deformation Mechanisms during Low- and High Temperature Superplasticity in 5083 Al-Mg Alloy," *METALLURGICAL AND MATERIALS TRANSACTIONS A*, vol. 33A, pp. 1373-1384, 2002.
  22. Strobel, K., Sweet, E., Easton, M., Feng Nie, J., & Coupe, M., "Dispersoid Phases in 6xxx Series Aluminium Alloys," *Materials Science Forum*, vol. 654 - 656, pp. 926-929, 2010.
  23. Rezaei Ashtiani, H. R., Parsa, M. H., Bisadi, H., "Effects of initial grain size on hot deformation behavior of commercial pure aluminum," *Materials & Design*, vol. 42, pp. 478-485, Dec. 2012.